E-Waste Based V_2O_5/RGO/Pt Nanocomposite for Photocatalytic Degradation of Oxytetracycline

Harshavardhan Mohan,[a,b] Dhanakumar Selvaraj,[b] Shanthi Kuppusamy,[b] Janaki Venkatachalam,[c] Yool-Jin Park,[d] Kamala-Kannan Seralathan,[a] and Byung-Taek Oh[a]

[a]Division of Biotechnology, Advanced Institute of Environment and Bioscience, College of Environmental and Bioresource Sciences, Chonbuk National University, Iksan Jeonbuk 54596, South Korea; kannan@jbnu.ac.kr, btoh@jbnu.ac.kr (for correspondence)

[b]Department of Environmental Science, PSG College of Arts and Science, Coimbatore 641 014, Tamil Nadu, India

[c]Department of Chemistry, Sri Sarada College for Women, Salem 636 016, Tamil Nadu, India

[d]Department of Ecology Landscape Architecture-Design, College of Environmental and Bioresource Sciences, Chonbuk National University, Iksan Jeonbuk 54596, South Korea

Published online 00 Month 2018 in Wiley Online Library (wileyonlinelibrary.com). DOI 10.1002/ep.13123

The increasing prevalence of antibiotics in the environment has promoted the development of antibiotic resistant microorganisms, and novel approaches are needed to effectively remove antibiotics from water and mitigate this worldwide problem. A reduced graphene oxide-V_2O_5 (RGOV) nanocomposite was synthesized and used for photocatalytic degradation of the antibiotic oxytetracycline (OTC) in aqueous solution. The Sol–Gel method was employed for V_2O_5 synthesis from e-waste-based vanadium nitrate, and a one pot solvothermal method was used to synthesize RGOV. Fourier-transform infrared spectroscopy (FTIR), X-ray diffraction spectroscopy (XRD), transmission electron microscopy (TEM) with energy dispersive analysis of X-rays (EDAX) confirmed V-O-C bonds on the surface of the RGOV nanocomposites. A decrease in the band gap of V_2O_5 from 2.21 to 2.13 eV was supported by diffuse reflectance ultraviolet–visible spectrophotometry. OTC adsorption onto the nanocomposite increased with an increase in RGO concentration and saturated at 17% for RGOV with 30% graphene oxide. The composite degraded 90% of the OTC present in aqueous solution (50 mg/L). Platinum (1%) doping further increased OTC degradation by the nanocomposite to 98.7%. Optimum conditions for maximum OTC degradation are (1) an initial OTC concentration of 50 mg/L, (2) a RGOV nanocomposite dose of 0.5 g/L, and (3) a 40 min incubation time. Our results support the potential use of RGOV nanocomposite for OTC photodegradation. © 2018 American Institute of Chemical Engineers Environ Prog, 2018

Keywords: E-waste, nanocomposite, oxytetracycline, photocatalytic degradation, RGO, vanadium pentoxide

INTRODUCTION

Antibiotics are extensively used in mariculture and animal farming to prevent bacterial infection and promote growth [1,2]. The increasing and in appropriate use (without proper veterinary guidance) of antibiotics is resulting in their entry into the environment at alarming levels, where they promote the development of multi-antibiotic resistant bacteria which disrupt natural microbial communities and adversely impact human and veterinary medical treatment [3,4]. Oxytetracycline (OTC) is a broad-spectrum antibiotic widely used for treating respiratory disorders, sexually transmitted infections, and other inflammatory diseases in animals [5]. Due to its affordability and minimal side effects, OTC has extensive use in animal husbandry. Problematically, nearly 70% of the compound is not metabolized and/or retained in the animal body and is excreted through urine and feces [6]. Aside from promoting antibiotic resistant microbes, OTC inhibits nitrification in aquatic systems, reduces biogas production during anaerobic digestion of manure, reduces microbial respiration, and decreases soil enzyme concentrations [7,8]. Several methods have been developed to decrease residual antibiotics in the environment. Heterogenous catalyst-based photocatalytic oxidation is one such method that has been proven to be highly effective [9].

Discarded electrical and electronic equipment are referred to as e-waste. E-waste contains substantial amounts of hazardous substances, which when leached into the environment pose serious threats to biological systems [10,11]. E-wastes are processed by recycling or removing hazardous components before they are accumulated for compacting and destruction. Numerous metal oxides are extracted from e-wastes, which when doped with photocatalysts tend to have higher photocatalytic activity [12].

V_2O_5 is one such metal oxide catalyst. It has a band energy gap of 2.47 eV and greater electron hole recombination when irradiated, thus demanding doping with transition metals and photocatalysts [13]. Graphene, having high adsorption capacity, conductivity and photo-conversion efficiency, serves as an ideal catalyst [14,15]. Hence, hybridization of V_2O_5 with reduced graphene oxide (RGO) yields high photocatalytic activity and stability even under natural irradiation, making it ideal for reuse over multiple cycles [16]. Additionally, doping with noble metals increases light adsorption in the visible light region due to greater surface excitation [17]. Among all the noble metals, platinum doping has been found to significantly increase the durability and electrocatalytic activity of the photocatalyst [18].

In this context, we present the findings of our study with following objectives: (1) synthesise V_2O_5 by the sol–gel method using vanadium nitrate extracted from e-waste; (2) dope V_2O_5 onto (RGO) graphene oxide; (3) characterize the synthesized

reduced graphene oxide-V_2O_5 (RGOV) nanocomposite; (4) assess the efficiency of the nanocomposite for OTC degradation; and (5) enhance the photocatalytic activity of the RGOV nanocomposite by platinum doping.

EXPERIMENTAL

Materials

Vanadium nitrate was obtained as a by-product of hydrometallurgical treatment of vanadium redox battery from an e-waste recycler in Coimbatore, Tamil Nadu, India. The other chemicals used in this experiment were procured from Sigma-Aldrich (India) and used as received.

Synthesis of V_2O_5 Nanoparticles

A metal citrate intermediate was prepared by constant stirring of a 2:1 ratio molar solution of vanadium nitrate solution and citric acid with 50 mL of water for 12 h at 45° C, then refluxing for 3 h. The metal citrate was chelated to the metal oxide to control particle size and ensure uniform distribution of the metal ion in the reaction mixture [19]. The reaction mixture was dried on a hot plate at 180–200° C for 60 min. The resultant V_2O_5 white powder was washed, dried in a vacuum oven at 60° C for 2 h, and used for further experiments.

Synthesis of Graphene Oxide

We adopted a modified Hummers method [20] for synthesis of graphene oxide (GO) from graphite powder. In brief, 2 g of graphite powder was gradually mixed in 100 mL of concentrated H_2SO_4 containing 8 g of $KMnO_4$ and stirred for 2 h. The temperature of the reaction mixture was maintained below 20° C using an ice bath with constant stirring for 30 min. Double-distilled water (100 mL) was added to the reaction mixture and stirred for another 15 min. The reaction was terminated by adding 200 mL of double-distilled water followed by 30 mL of 30% H_2O_2 aqueous solution. The solid product was separated by centrifugation and washed repeatedly with 5% HCl in water until the pH of the supernatant solution became neutral. The brown solid was vacuum dried at 60° C before use.

Synthesis of Reduced Graphene Oxide Vanadium Oxide (RGOV)

A RGOV composite was prepared using a solvothermal process. In brief, GO (0.2, 0.4, and 0.6 g to obtain 10%, 20%, and 30% w/w, respectively) was sonicated in 50 mL methanol for 30 min at room temperature to achieve uniform dispersion. Synthesized V_2O_5 (2 g) was gradually added to the flask and the reaction mixture was stirred mechanically for 1 h to ensure complete mixing. The homogeneous suspension was transferred to a Teflon-lined stainless steel autoclave and placed in a hot air oven at 120° C for 8 h, where reduction of GO to RGO was facilitated by autogenous pressure generated within the vessel. The pressure simultaneously enhanced the merging of V_2O_5 onto RGO layers. The resulting composite was washed repeatedly with water, filtered, dried in vacuum at 60° C, and stored in a desiccator until use. The prepared materials were labeled RGOV-10, RGOV-20, and RGOV-30.

Platinum Doping of RGOV-20

Platinum chloride was used as the precursor for platinum metal. Briefly, 2.5 mg of platinum chloride and 2 g of RGOV-20 were added to a beaker containing 30 mL of double-distilled water. The reaction mixture was stirred vigorously at 80° C until it became dry. The dried mixture was scraped and reduced with hydrogen gas at 450° C. The prepared catalyst was labeled RGOV-20/Pt (1%).

Characterization

After pelleting with KBr, Fourier-transform infrared spectra were obtained in transmission mode on a Shimadzu DR-8101A Spectrophotometer. A Philips X'Pert Pro MPD diffractometer was used to perform X-Ray Diffraction analysis with Cu radiation between 5 and 80° 2θ at a scan rate of 0.1°/min and an incident wavelength of 0.154 nm. An aqueous solution of the sample was deposited in micro grids to ascertain morphology and composition using transmission electron microscopy and energy dispersive X-ray (Hitachi JEOL-2010 HRTEM). Spectra were also obtained with a UV–visible diffuse reflectance spectrophotometer (Jasco V650) with an integrated sphere assembly using $BaSO_4$ as the reference.

Photocatalytic Studies

Photocatalytic activity of the RGOV nanocomposite towards OTC degradation was assessed using an immersion well batch photoreactor. A known amount of catalyst was dispersed in an aqueous solution of OTC at the desired concentration under ultrasonication for 5 min. Before irradiating, the suspensions were stirred in the dark for 20 min to equilibrate OTC adsorption on the catalyst surfaces. A 150 W xenon lamp was used as the irradiation source. During irradiation, 0.2 mL aliquots were withdrawn at regular time intervals and centrifuged at 8,000 rpm for 5 min. OTC degradation was quantified based on the change in concentration with time, determined using a total organic carbon analyzer (TOC-V CSH Analyzer Shimadzu). OTC adsorption onto the nanocomposite (in the absence of light) was evaluated using the same procedure. OTC photolysis was also determined using the xenon lamp in the absence of catalyst. OTC removal percentage was calculated:

$$\text{Degradation}\ (\%) = \frac{(C_0 - C_t)}{C_0} \times 100 \quad (1)$$

where, C_O is the initial concentration of OTC and C_t is OTC concentration at various time intervals.

Recycling of the Catalyst

After treatment, the OTC solution and photocatalyst were left undisturbed for 1 h. The supernatant was then decanted and the composite separated by filtration, washed with deionized water, vacuum dried at 60° C, and reused for subsequent photocatalysis experiments.

RESULTS AND DISCUSSION

Characterization

Fourier-Transform Infrared Spectroscopy

In the Fourier-transform infrared spectroscopy (FTIR) spectrum of the synthesized V_2O_5 nanoparticle [Figure 1(a)], the broad absorption band at 1020–853 cm^{-1} was attributed to V=O stretching and a peak at 480 cm^{-1} to V-O-V bonding. This adsorption band matched that of a previous study [18]. Peaks corresponding the oxygen-containing functional groups of carboxylate (C–O) at 1050 cm^{-1}, epoxide (C–O–C) at 1225 cm^{-1}, C–OH deformation peak at 1380 cm^{-1}, and C–O stretching of COOH groups at 1700 cm^{-1} were well defined in the FTIR spectra of the GO and RGOV composites. The sharp peak at 1624 cm^{-1} and the broad band at 3600 cm^{-1} are indicators of adsorbed water on hydrophilic GO [12]. No additional peaks were observed in the FTIR spectrum of the RGOV-20/Pt (1%) composite, attesting to the low platinum concentration.

X-Ray Diffraction Spectroscopy

Figure 1b shows the structural characterization of the RGOV, RGO, and RGOV-20/Pt(1%) nanocomposites. A sharp diffraction peak at 2θ = 10.2° originated from RGO, is in good agreement with a previous study [21]. The x-ray diffraction

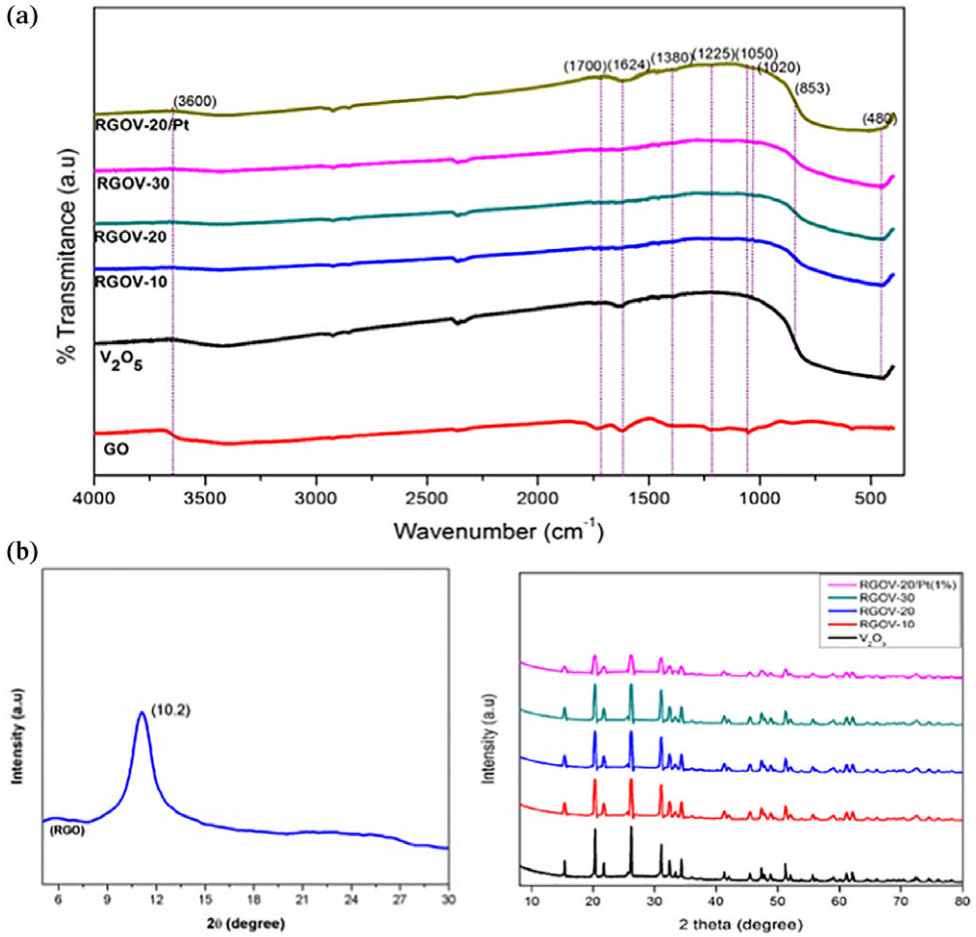

Figure 1. (a) FTIR spectra of GO, V_2O_5, RGOV (10, 20 & 30) and RGOV-20/Pt (1%) photocatalysts; (b) XRD spectra of GO, V_2O_5, RGOV (10, 20 & 30) and RGOV-20/Pt (1%) photocatalysts. [Color figure can be viewed at **wileyonlinelibrary.com**]

spectroscopy (XRD) spectrum of V_2O_5 indicates that the synthesized photocatalyst is crystalline in nature. Good matching with JCPDS Number 09–0387 with attributed (h k l) values of 200, 001, 110, 400, 011, 310, 002, 411, 600, 601, 121, 420, and 710 is a further indicator of crystallinity [22]. Similar XRD spectra were obtained for all of the prepared photocatalysts, inferring that the crystalline structure of V_2O_5 is not significantly impacted by RGO loading and platinum doping.

Transmission Electron Microscopy

Transmission electron microscopy (TEM) and EDAX were performed to study the morphology and the composition of the prepared sample [Figure 2(a–e)]. The RGO electron micrograph showed thin stacked flakes with a few well-defined structural layers at the edges. The TEM image indicated that the nanocomposite was devoid of particle agglomeration and had a uniform structure with controlled particle size. The composite also had a uniform deposition of V_2O_5 and Pt (1%) metal over the RGO surface with no separate particle over the edges insuring the absence of blends but strong bonds with RGO sheets. The presence of C (23.87%), V (49.61%), O (25.42%) and Pt (1.10%) was determined by EDAX mapping of the RGOV 20/Pt composite. The absence of impurities indicated that the synthesized photocatalyst was of very high purity.

DRS-UV

Diffuse reflectance spectra (DRS) of V_2O_5, RGOV-20, and RGOV-20/Pt (1%) are shown in Figure 2f. The band gap of the synthesized V_2O_5 was 2.21 eV. However, the band gap of RGOV-20 decreased to 2.13 eV, indicating strong interaction between V_2O_5 and RGO sheets. Doping with transition metal Pt (1%) further decreased the band gap to 2.09 eV. Thus, the introduction of RGO improves the light absorption capacity of V_2O_5 in the visible light region compared to bare V_2O_5 and loading with Pt (1%) further enhanced the conducting nature of the composite.

Photocatalytic Studies

OTC Adsorption

OTC adsorption onto the nanocomposite surfaces in darkness is shown in Figure 3. The maximum adsorption OTC on V_2O_5 was 8%, whereas for RGOV adsorption increased with increasing RGO content and became saturated at 17% for RGOV-30. This can be attributed to hydrogen bonding between OTC and surface hydroxyl groups. For all catalysts, adsorption–desorption equilibrium was attained at 20 min [23].

Effect of RGO (%) and Pt (1%) on OTC Degradation

The optimum weight (%) of RGO (w/w) with respect to V_2O_5 for maximum degradation of OTC was determined [Figure 4(a)]. The degradation efficiency of bare V_2O_5 was 58% after 60 min, while RGOV-10 had a degradation efficiency of 68% and RGOV-20 had an even greater efficiency of 90%. A further increase in RGO content from 20 to 30% did not significantly increase OTC degradation. Thus, subsequent experiments to optimize photocatalytic parameters were conducted with the RGOV-20 nanocomposite. The electronic interaction

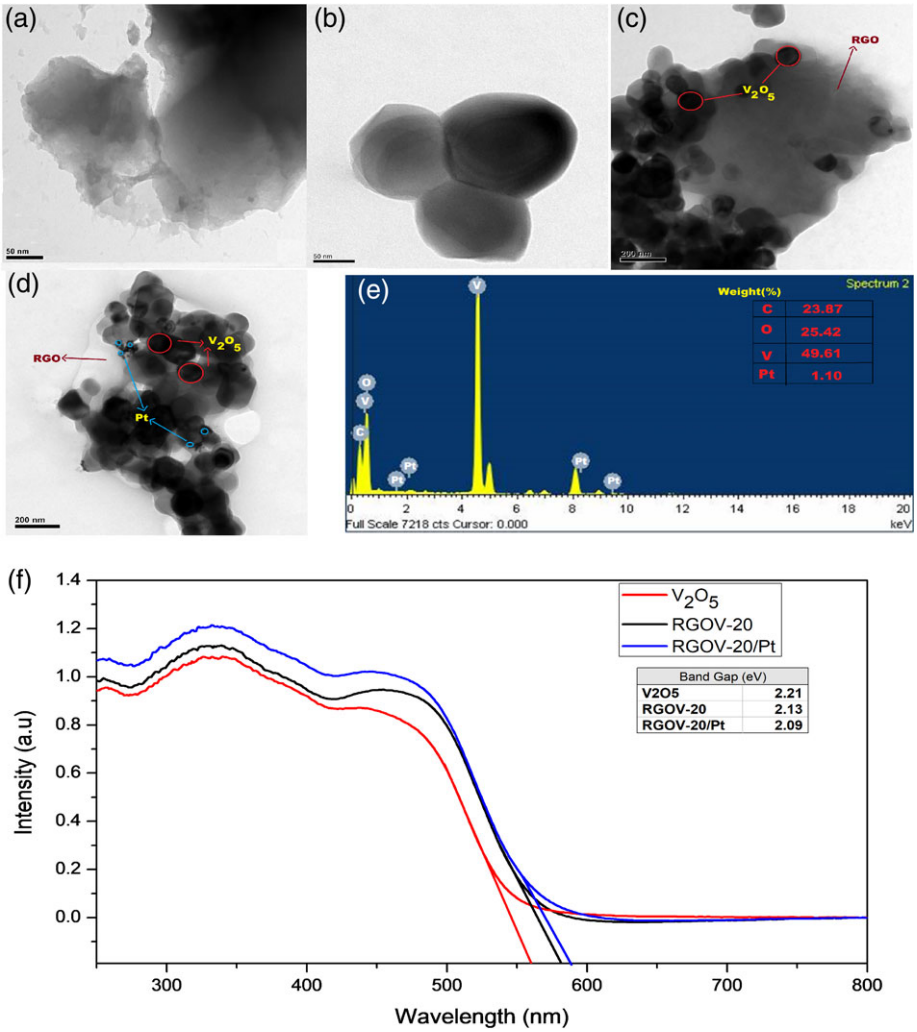

Figure 2. (a) TEM image of (a) RGO, (b) V_2O_5, (c) RGOV-20, (d) RGOV-20/Pt (1%), and (e) EDAX Spectrum of RGOV-20/Pt (1%) photocatalyst; (f) DRS-UV spectra of V_2O_5, RGOV-20 and RGOV-20/Pt (1%) photocatalysts. [Color figure can be viewed at **wileyonlinelibrary.com**]

of RGO with V_2O_5 has been found to retard the recombination of photo-induced charge carriers by prolonging electron lifetime, promoting generation of oxy reactive species and capturing photo-generated holes. This can be attributed to the enhanced catalytic activity of RGOV [24].

Doping with 1% Pt [Figure 4(b)] improved OTC degradation (98% after 40 min). Thus, the RGOV-20/Pt(1%) nanocomposite proved to be an efficient photocatalyst for OTC degradation. The enhanced degradation can be attributed to the conducting ability of the platinum metal, which further decreases electron hole recombination [18].

OTC Concentration

Photocatalytic degradation of OTC on RGOV-20/Pt(1%) was determined at different initial concentration (25–100 mg/L) and the results are shown in Figure 4c. Degradation decreased with increasing OTC concentration. Maximum degradation was observed at lower initial concentrations (25 and 50 mg/L) and as initial concentration increased, degradation decreased. At an initial concentration of 100 mg/L, degradation was 40%. This phenomenon is mainly attributed to the fact that the color intensity of OTC solution tends to increase with increase in OTC concentration. The higher the color intensity the lesser would be the ability of light to penetrate deep into the solution and excite electrons, thus, resulting in decreased degradation rates [25]. Under the conditions of the experiment degradation was maximal at 50 mg OTC/L.

RGOV-20 Pt(1%) Dosage

Catalyst dosage should be optimized for photocatalysis to avoid using excessive amounts of catalyst. Degradation of OTC at 50 mg/L was determined at catalyst doses of 0.25, 0.5, 0.75, and 1 g/L [Figure 4(d)]. OTC degradation increased from 90% to 98.7% with an increase in catalyst dosage from 0.25 to 0.5 g/L. Further increases in catalyst dosage (0.75 and 1 g/L) did not increase degradation. This is due in part to an increase in agglomeration of nanocomposites, which makes the solution more turbid. Higher turbidity increases light scattering, which negatively affects photocatalytic degradation efficiency [26]. Degradation (upto 58%) was rapid in the initial 10 min of the reaction, indicating sufficient reactive sites in 50 mg of the nanocomposite. Further studies should address the influence

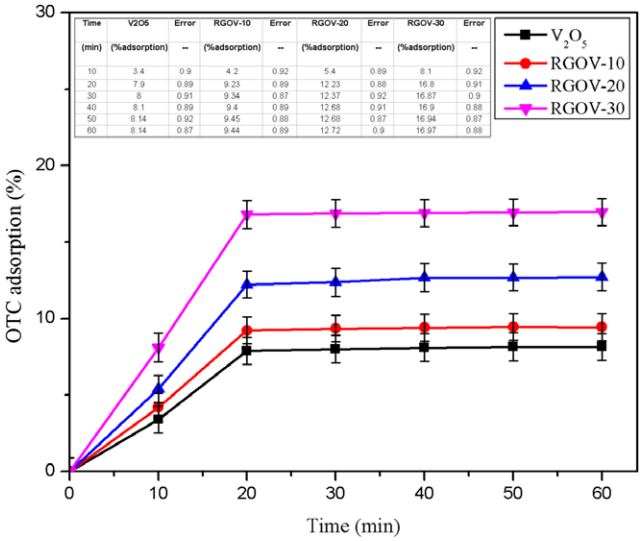

Figure 3. Adsorption of OTC over different catalysts (Experimental condition: Initial OTC concentration of 50 mg/L and catalytic dose: 0.5 g/L in dark). [Color figure can be viewed at **wileyonlinelibrary.com**]

of salts and metals on the photocatalytic activity of the RGOV-20 nanocomposite.

Kinetics of OTC Degradation

The photocatalytic degradation of OTC was well-described by pseudo-first order kinetics, following the Langmuir–Hinshelwood model [27]:

$$R = \frac{-dC_0}{dt} = \frac{k_r K C_0}{1 + K C_0} \tag{2}$$

Upon integration and elimination of insignificant elements from (2),

$$ln\left(\frac{C_0}{C}\right) = k't \tag{3}$$

where, k′ is the apparent rate constant (min^{-1}) of the photocatalytic degradation. A plot of ln (*Co/C*) *versus* time (min) yields a straight line and the slope is the degradation rate. Figure 5a shows OTC degradation kinetics under optimized conditions. The degradation rate constant was 1.878×10^{-2} min^{-1}.

Catalyst Stability and Reusability

Reusability and stability of the catalyst is essential for practical applications [28]. Repeated OTC photodegradation experiments were performed to estimate the reusability of RGOV-20/Pt(1%) as a photocatalyst. Results [Figure 5(b)] suggest that RGOV-20/Pt(1%) can be reused for four cycles, as only an 11% reduction in OTC degradation was observed between the first and fourth cycle. This indicates high stability, although additional research should be conducted to further increase the reusability of the photocatalyst.

CONCLUSION

The RGOV-20 nanocomposite prepared by a solvothermal method degraded 90% of OTC compared to bare V_2O_5 (58%) within 60 min. Increasing RGO loading in excess of 20% did not significantly impact OTC degradation. On doping with Pt 1%, OTC degradation increased to 98.7% within 40 min, thus demonstrating high potential of RGOV-20/Pt(1%) for OTC removal.

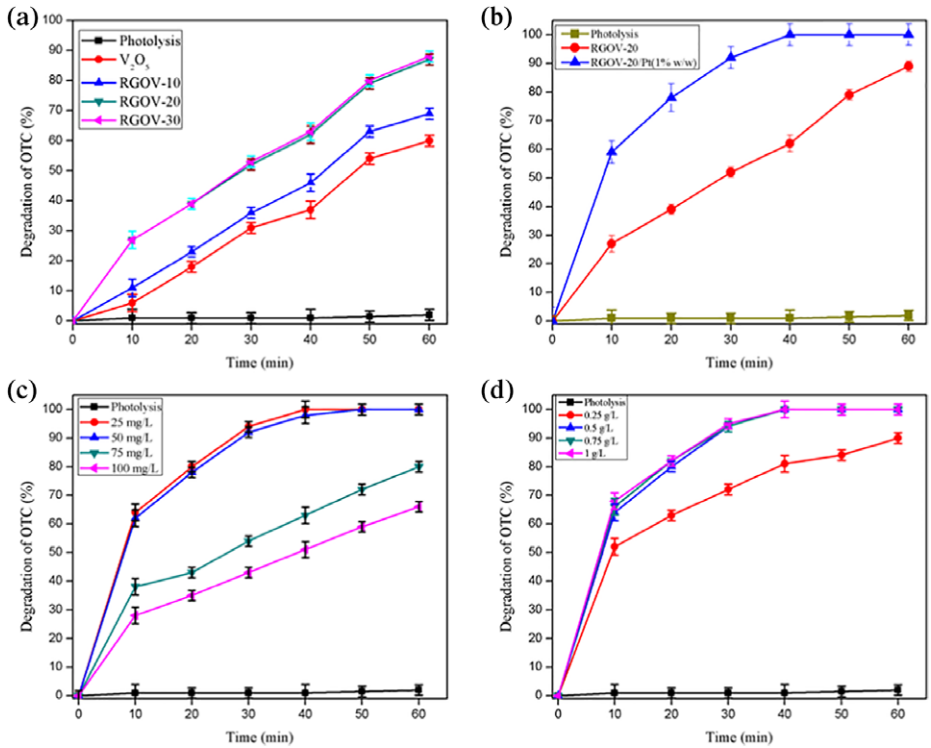

Figure 4. (a) Effect of RGO loading of the catalyst; (b) improved efficiency on doping Pt (1%) on the degradation of OTC (Experimental condition: Initial OTC concentration of 50 mg/L and catalytic dose: 0.5 g/L); (c) Effect of initial concentration over the degradation of OTC for RGOV-20; (d) Effect of weight of the catalyst on the degradation of OTC. [Color figure can be viewed at **wileyonlinelibrary.com**]

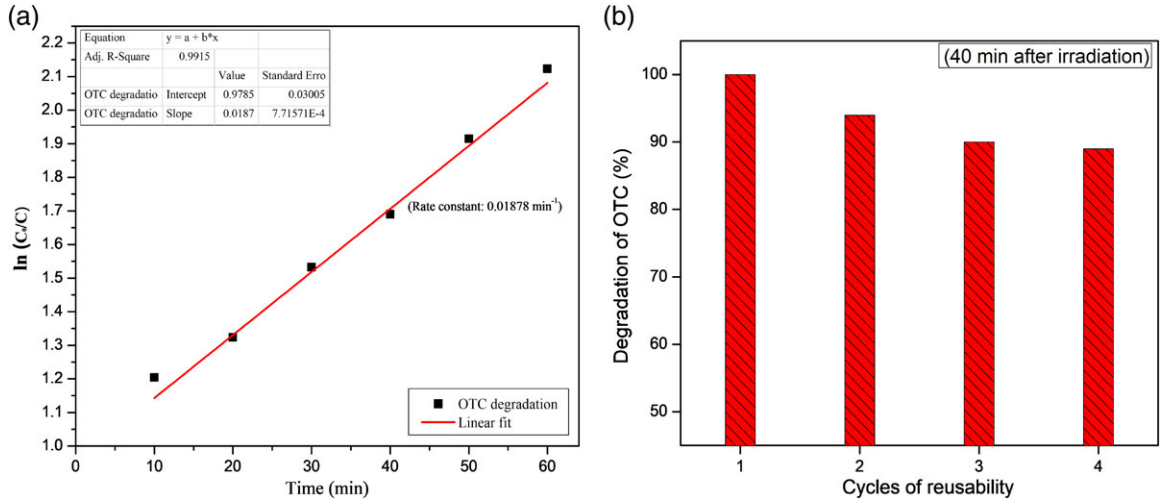

Figure 5. (a) OTC degradation kinetics of RGOV-20/Pt (1% w/w) photocatalyst; (b) Reusability of RGOV-20/ Pt (1% w/w) photocatalyst. [Color figure can be viewed at **wileyonlinelibrary.com**]

ACKNOWLEDGMENTS

This research was supported by the BK21 plus program through the National Research Foundation (NRF) funded by the Ministry of Education of Korea. Authors are grateful to Dr. Patrick J. Shea, Professor, School of Natural Resources, University of Nebraska-Lincoln, Lincoln, NE 68583-0817, USA, for fine tuning of the manuscript.

LITERATURE CITED

1. Grenni, P., Ancona, V., & Caracciolo, A.B. (2018). Ecological effects of antibiotics on natural ecosystems: A review, Microchemical Journal, 136, 25–39.
2. Li, S., Zhang, S., Ye, C., Lin, W., Zhang, M., Chen, L., Li, J., & Yu, X. (2017). Biofilm processes in treating mariculture wastewater may be a reservoir of antibiotic resistance genes, Marine Pollution Bulletin, 118, 289–296.
3. Woegerbauer, M., Zeinzinger, J., Gottsberger, R.A., Pascher, K., Hufnagl, P., Indra, A., Fuchs, R., Hofrichter, J., Kopacka, I., Korschineck, I., & Schleicher, C. (2015). Antibiotic resistance marker genes as environmental pollutants in GMO-pristine agricultural soils in Austria, Environmental Pollution, 206, 342–351.
4. Gothwal, R., & Shashidhar, T. (2015). Antibiotic pollution in the environment: a review, Clean—Soil, Air, Water, 43, 479–489.
5. Yeom, J.R., Yoon, S.U., & Kim, C.G. (2017). Quantification of residual antibiotics in cow manure being spread over agricultural land and assessment of their behavioral effects on antibiotic resistant bacteria, Chemosphere, 182, 771–780.
6. Turker, G., Akyol, Ç., Ince, O., Aydin, S., & Ince, B. (2018). Operating conditions influence microbial community structures, elimination of the antibiotic resistance genes and metabolites during anaerobic digestion of cow manure in the presence of oxytetracycline, Ecotoxicology and Environmental Safety, 147, 349–356.
7. Jiménez-Gamboa, D., Castro-Gutiérrez, V., Fernández-Fernández, E., Briceño-Guevara, S., Masís-Mora, M., Chin-Pampillo, J.S., Mora-López, M., Carazo-Rojas, E., & Rodríguez-Rodríguez, C.E. (2018). Expanding the application scope of on-farm biopurification systems: Effect and removal of oxytetracycline in a biomixture, Journal of Hazardous Materials, 342, 553–560.
8. Zhang, Y., Zhang, C., Parker, D.B., Snow, D.D., Zhou, Z., & Li, X. (2013). Occurrence of antimicrobials and antimicrobial resistance genes in beef cattle storage ponds and swine treatment lagoons, Science of the Total Environment, 463, 631–638.
9. Maruthamani, D., Divakar, D., & Kumaravel, M. (2015). Enhanced photocatalytic activity of TiO_2 by reduced graphene oxide in mineralization of Rhodamine B dye, Journal of Industrial and Engineering Chemistry, 30, 33–43.
10. Perkins, D.N., Drisse, M.N.B., Nxele, T., & Sly, P.D. (2014). E-waste: a global hazard, Annals of Global Health, 80, 286–295.
11. Singh, M., Thind, P.S., & John, S. (2018). Health risk assessment of the workers exposed to the heavy metals in e-waste recycling sites of Chandigarh and Ludhiana, Punjab, India, Chemosphere, 203, 426–433.
12. Xie, X.D., Zhou, K., Chen, B.Y., & Chang, C.T. (2016). Degradation of oxytetracycline using microporous and mesoporous photocatalyst composites: Uniform design to explore factors, Journal of Environmental Chemical Engineering, 4, 4453–4465.
13. Suresh, R., Giribabu, K., Manigandan, R., Munusamy, S., Kumar, S.P., Muthamizh, S., Stephen, A., & Narayanan, V. (2014). Doping of Co into V_2O_5 nanoparticles enhances photodegradation of methylene blue, Journal of Alloys and Compounds, 598, 151–160.
14. Okoth, O.K., Yan, K., & Zhang, J. (2017). Mo-doped $BiVO_4$ and graphene nanocomposites with enhanced photoelectrochemical performance for aptasensing of streptomycin, Carbon, 120, 194–202.
15. Liu, X., Zeng, J., Yang, H., Zhou, K., & Pan, D. (2018). V_2O_5-Based nanomaterials: synthesis and their applications, RSC Advances, 8, 4014–4031.
16. Boruah, P.K., Szunerits, S., Boukherroub, R., & Das, M.R. (2018). Magnetic Fe_3O_4@ V_2O_5/rGO nanocomposite as a recyclable photocatalyst for dye molecules degradation under direct sunlight irradiation, Chemosphere, 191, 503–513.
17. Ambrožová, N., Reli, M., Šihor, M., Kuśtrowski, P., Wu, J. C., & Kočí, K. (2018). Copper and platinum doped titania for photocatalytic reduction of carbon dioxide, Applied Surface Science, 430, 475–487.
18. Anwar, M.T., Yan, X., Shen, S., Husnain, N., Zhu, F., Luo, L., & Zhang, J. (2017). Enhanced durability of Pt electrocatalyst with tantalum doped titania as catalyst support, International Journal of Hydrogen Energy, 42, 30750–30759.
19. Sridhar, C., Gunvanthrao Yernale, N., & Prasad, M.V.N. (2016). Synthesis, spectral characterization, and antibacterial and antifungal studies of PANI/V_2O_5 nanocomposites,

International Journal of Chemical Engineering, Article ID 3479248.
20. Jia, W., Li, Z., Wu, Z., Wang, L., Wu, B., Wang, Y., Cao, Y., & Li, J. (2018). Graphene oxide as a filler to improve the performance of PAN-$LiClO_4$ flexible solid polymer electrolyte, Solid State Ionics, 315, 7–13.
21. Romero, A., Lavin-Lopez, M.P., Sanchez-Silva, L., Valverde, J. L., & Paton-Carrero, A. (2018). Comparative study of different scalable routes to synthesize graphene oxide and reduced graphene oxide, Materials Chemistry and Physics, 203, 284–292.
22. Ashour, A., & El-Sayed, N.Z. (2009). Physical properties of V_2O_5 sprayed films, Journal of Optoelectronics and Advanced Materials, 11, 251–256.
23. Li, K., Xiong, J., Chen, T., Yan, L., Dai, Y., Song, D., Lv, Y., & Zeng, Z. (2013). Preparation of graphene/TiO_2 composites by nonionic surfactant strategy and their simulated sunlight and visible light photocatalytic activity towards representative aqueous POPs degradation, Journal of Hazardous Materials, 250, 19–28.
24. Shanmugam, M., Alsalme, A., Alghamdi, A., & Jayavel, R. (2015). Enhanced photocatalytic performance of the graphene-V_2O_5 nanocomposite in the degradation of methylene blue dye under direct sunlight, ACS Applied Materials & Interfaces, 7, 14905–14911.
25. Heidari, S., Haghighi, M., & Shabani, M. (2018). Ultrasound assisted dispersion of Bi_2 Sn_2O_7-C_3N_4nanophotocatalyst over various amount of ZeoliteY for enhanced solar-light photocatalytic degradation of tetracycline in aqueous solution, Ultrasonics Sonochemistry, 43, 61–72.
26. Maruthamani, D., Divakar, D., Harshavardhan, M., & Kumaravel, M. (2018). Evaluation of bactericidal activity of reduced graphene oxide supported titania nanoparticles under visible light irradiation, Journal of Chemical and Pharmaceutical Research, 8, 236–244.
27. Turolla, A., Bestetti, M., & Antonelli, M. (2018). Optimization of heterogeneous photoelectrocatalysis on nanotubular TiO_2 electrodes: Reactor configuration and kinetic modelling, Chemical Engineering Science, 182, 171–179.
28. Mäsing, F., Wang, X., Nüsse, H., Klingauf, J., & Studer, A. (2017). Facile light-mediated preparation of small polymer-coated palladium-nanoparticles and their application as catalysts for alkyne semi-hydrogenation, Chemistry: A European Journal, 23, 6014–6018.